Enhancing Broadside Focusing in 6G Near-Field Communications Using HOBFs within UCCA

Gamal M. Alausta[1] ,Mohammed N. Mohammed[2]
[1.2]Department of Electrical and Electronics Engineering, Tripoli University, Libya
[1]g.alausta@uot.edu.ly, [2]modenaser108@gmail.com

***Abstract*— The ability of antenna arrays to achieve sharp broadside focusing is pivotal for near-field communications in sixth-generation (6G) systems, where Extremely Large-Scale Antenna Arrays (ELAAs) are envisioned as a core technology. Although Uniform Concentric Circular Arrays (UCCAs) have been demonstrated to outperform conventional Uniform Circular Arrays (UCAs) in extending the near-field region-mainly by exploiting zero- and first-order Bessel functions-the role of higher-order Bessel functions ($\mathbf{HOBFs}, \mathbf{J_n(\cdot), n > 1}$) has received limited attention. This paper introduces a comprehensive analytical framework that systematically incorporates HOBFs to refine the broadside focusing capability of UCCAs. Through mathematical derivations and numerical evaluations, it is shown that HOBFs contribute additional degrees of freedom for beam pattern control, leading to more accurate depth focusing, flexible beam shaping, and enhanced user separation. The analysis reveals that the integration of HOBFs significantly enlarges the Effective Rayleigh Distance (ERD) and reduces inter-user interference, thereby improving spatial resolution and system robustness. These findings highlight the potential of HOBF-assisted UCCAs as a cornerstone in designing near-field multi-user multiple-input multiple-output (MIMO) systems for 6G. The proposed methodology provides theoretical insights and practical guidelines for future beamforming strategies aimed at overcoming the challenges of dense deployments, interference mitigation, and high-capacity demands.**

Keywords—6G, Near-Field Communications, ELAAs, UCCAs, HOBFs, Beam Focusing, Broadside Enhancement.

1. Introduction

The relentless demand for ultra-high data rates, massive connectivity, and low latency is driving the transition toward sixth-generation (6G) wireless networks, where Extremely Large-Scale Antenna Arrays (ELAAs) are anticipated to play a central role [1]. With hundreds or even thousands of antenna elements integrated into such arrays, the conventional far-field assumption governed by planar wavefronts collapses, as the radiating near-field (Fresnel) region may extend to several hundred meters [2]. Consequently, Near-Field Communications (NFC) emerge as a foundational paradigm in 6G system design, allowing not only angular beam steering but also spatially precise beam focusing. This unique feature enables depth multiplexing, where multiple users can be distinguished not only by angle but also by distance [3].Among various focusing scenarios, the broadside direction (perpendicular to the array plane) is of special interest because of its symmetric coverage properties. Traditional Uniform Circular Arrays (UCAs) have been extensively studied for their 360° coverage and geometric simplicity [4]. However, their beam pattern in the broadside region is dominated by the zero-order Bessel function (J_0), which inherently limits focus depth control and sidelobe suppression. To address this issue, researchers proposed Uniform Concentric Circular Arrays (UCCAs), composed of multiple concentric rings, which demonstrated improved broadside focusing through the constructive combination of J_0 and the first-order Bessel function (J_1) [5]. Similar approaches, such as frequency diverse arrays (FDAs), have also been investigated to enhance near-field focusing efficiency [6].

Beyond classical array theory [4], recent advances in millimeter-wave and massive MIMO communications have underscored the potential of large-scale and near-field beamforming [7][8][9]. For instance, studies on intelligent surfaces and extremely large aperture arrays highlighted the importance of exploiting spherical wavefronts to unlock higher spatial resolution [10-11]. Furthermore, practical applications in backhaul, UAV-assisted links, and hybrid beamforming architectures emphasize the need for robust near-field beam focusing strategies that mitigate interference and improve spectral efficiency [12-14].

Despite these advancements, one major research gap persists: the explicit role of higher-order Bessel functions (HOBFs, $J_n(\cdot)$, $n > 1$) in UCCA beamforming has been largely neglected. While HOBFs naturally appear in the analytical expansion of UCCA responses, they are often disregarded for mathematical simplicity. This oversight overlooks their potential to improve beam shaping, depth focusing, and interference suppression. Addressing this gap is crucial, as the mathematical properties of HOBFs-including their orthogonality-like behavior and distinct sidelobe structures-may provide powerful tools for multi-user separation in dense near-field scenarios [15].

2. System Model

The system model considers a downlink Extremely ELAA millimeter-wave (mmWave) communication system, where the BS is equipped with a UCCA to serve multiple single-antenna users. The UCCA is composed of multiple uniform circular arrays (UCAs) with different radii, where antennas are uniformly distributed along each circular periphery. The radius

DOI:10.5281/zenodo.17540622

of each concentric UCA is proportional to its index, which ensures uniform spatial coverage and efficient utilization of the array aperture.

2.1 Multipath channel model for the *m*-th UCA

In the considered downlink mmWave ELAA system, a UCCA at the BS serves a single- antenna user. The channel between the m-th UCA and the user is modeled as a sum of L resolvable paths, each contributing a complex gain and a beam-steering vector evaluated at its elevation and azimuth.

$$h_m = \sum_{l=1}^{L} g_l \; a_m(\theta_l, \phi_l) \qquad (2.1)$$

Where

- h_m : Channel between the m-th UCA and the user.
- L : Number of resolvable paths between the BS and the user.
- g_l : Complex gain of the l-th path.
- θ_l : Elevation angle of the l-th path.
- ϕ_l : Azimuth angle of the l-th path.
- $a_m(\theta, \phi)$: Beam-steering vector of the m-th UCA for direction (θ, ϕ).
- m : Index of the UCA ring within the UCCA, with $m = 1,2, \dots, M$.

2.2 Second-order Taylor approximation of the element–user distance for the *n*-th antenna on the *m*-th UCA

This approximation expands the spherical path length into a second-order Taylor series, yielding a closed-form expression suitable for near-field analysis of UCAs. It enables tractable phase modeling per element when the user is at a finite range.

$$r_m^{(n)} = \sqrt{r^2 + R_m^2 - 2rR_m \sin\theta \cos(\phi - \psi_n)} \qquad (2.2)$$

where

- $r_m^{(n)}$: distance from the user to the n-th element on the m-th UCA.
- r : distance from the user to the UCCA center.
- R_m : radius of the m-th UCA.
- θ, ϕ : elevation and azimuth of the user, respectively.
- $\psi_n = 2\pi n / N_m$: azimuth of element n on the m-th UCA.
- N_m : number of antennas on the m-th UCA; $n = 1, \dots, N_m$.
- (a): second-order Taylor approximation.

2.3Distance-domain beamforming gain for the *m*-th UCA

When the angular directions match, the near-field gain of a single circular subarray depends only on the range difference and follows a zero-order Bessel profile.

$$G_m(\Theta_1, \Theta_2) = \mathbf{b}_m^H(r_1, \theta, \phi)\, \mathbf{b}_m(r_2, \theta, \phi) \approx J_0(|\xi|) \quad (2.3)$$

$$\xi = \frac{\pi R_m^2 \sin^2\theta}{2\lambda}\left(\frac{1}{r_1} - \frac{1}{r_2}\right) \qquad (2.4)$$

where

- $G_m(\Theta_1, \Theta_2)$: Beamforming gain between two range points for the m-th UCA.
- $\Theta_i = (r_i, \theta, \phi)$: User/focus location with aligned angles.
- $\mathbf{b}_m(\cdot)$: Near-field steering vector of the m-th UCA.
- J_0 : Zero-order Bessel function of the first kind.
- ξ : Bessel argument given above.
- R_m : Radius of the m-th UCA.
- λ : Wavelength.
- θ, ϕ : Elevation and azimuth.
- r_1, r_2 : Ranges of the two points.

2.4 Near-field UCCA gain via per-ring Bessel reduction

Starting from the exact inner product $G(\Theta_1, \Theta_2) = |\mathbf{b}H(r_1, \theta, \phi)\, \mathbf{b}(r_2, \theta, \phi)|$, the element- wise phase is split into a ring-dependent term and a cosine term; applying the Jacobi–Anger expansion collapses the per-ring element sum to $N_m J_0(\xi)$, yielding the compact summation below.

$$G(\Theta_1, \Theta_2) \approx \frac{1}{N}\left|\sum_{m=1}^{M} e^{-j\frac{\alpha\theta_m^2}{2}\left(1-\frac{1}{2}\sin^2\theta\right)\left(\frac{1}{r_1}-\frac{1}{r_2}\right)} N_m J_0(\xi)\right| \qquad (2.5)$$

where

- $G(\Theta_1, \Theta_2)$: near-field gain overlap between two points $\Theta_i = (r_i, \theta, \phi)$.
- $\mathbf{b}(r, \theta, \phi)$: spherical-wave steering vector of the array.
- R_m : radius of the m-th UCA
- N_m : number of antennas on the m-th UCA
- M : number of UCAs
- $N = \sum_{m=1}^{M} N_m$.
- λ : wavelength
- J_0 : zeroth-order Bessel function of the first kind.
- r_1, r_2 : ranges from the array center to Θ_1, Θ_2

θ, ϕ : elevation and azimuth

2.6 Broadside closed-form gain of UCCA (sinc form)

Special case of Eq. (2.6) at θ = 0. Under a large number of rings, the per-ring sum reduces to a closed form proportional to a sinc function.

$$G(\Theta_1, \Theta_2)|_{\theta=0} \approx \frac{1}{\zeta}\left|e^{-j\zeta} - 1\right| = \frac{|\sin(\zeta/2)|}{\zeta/2} \qquad (2.6)$$

where

- $G(\Theta_1, \Theta_2)$: near-field gain overlap between two points $\Theta_i = (r_i, \theta, \phi)$.
- $\theta = 0$: broadside direction.
- $\zeta = \frac{\pi R_{\max}^2}{\lambda}\left(\frac{1}{r_1} - \frac{1}{r_2}\right)$.
- $R_{\max}$: radius of the outermost UCA in the UCCA.
- λ : wavelength
- r_1, r_2 : ranges from array center to Θ_1, Θ_2.

2.7 Coplanar closed-form beamforming gain of UCCA

Special case of the near-field UCCA gain when users lie in the array plane, θ = π/2. Under a large number of rings, the per-ring sum reduces to a compact Bessel-form expression.

$$G(\Theta_1, \Theta_2)|_{\theta=\pi/2} \approx \sqrt{J_0^2\left(\frac{\zeta}{2}\right) + J_1^2\left(\frac{\zeta}{2}\right)} \quad (2.7)$$

where

- $G(\Theta_1, \Theta_2)$: gain overlap between two points $\Theta_i = (r_i, \theta, \phi)$.
- $\theta = \pi/2$: coplanar direction with respect to the array.
- J_0,J_1 : zeroth- and first-order Bessel functions of the first kind.
- $\zeta = \frac{\pi R_{\max}^2}{\lambda}\left(\frac{1}{r_1} - \frac{1}{r_2}\right)$, with $R_{\max}$ the outermost UCA radius, λ the wavelength, and r_1, r_2 the ranges from the array center to Θ_1, Θ_2.

In traditional UCA (Uniform Circular Array) systems, a major limitation lies in the restricted broadside focusing capability, where the beamforming effectiveness in the near-field region is reduced, leading to high ripple and degraded performance in critical areas. Moreover, the minimum floor (Min-floor) value was relatively low, further weakening the system's performance at critical points. The UCCA (Uniform Concentric Circular Array) partially addressed this issue by expanding the near-field region and improving the radial distribution of signals, yet it still suffers from limitations in precisely controlling signal ripple and reducing the inter-sidelobe level (ISL), particularly when enhanced focusing is required at specific points. The introduction of BMix-3 and BMix-5 overcomes these challenges by employing high-order combinations of multiple Bessel functions with tuning coefficients to control the relative contribution of each order. This approach achieves superior focusing, reduced ripple, and lower ISL compared to UCA and UCCA, while also significantly increasing the Min-floor, thereby enhancing performance in critical regions and ensuring more stable and higher-quality signal characteristics.

2.8 BesselMix

In the field of signal processing and antenna array design, Bessel functions play a critical role in describing wave propagation in circular and cylindrical geometries. Traditional approaches, such as using the zero-order Bessel function $J_0(\zeta)$, provide a fundamental model for near-field focusing and beamforming. However, single-order Bessel functions often exhibit limitations in controlling sidelobe levels, ripple characteristics, and near-field focusing precision.

To overcome these limitations, the BesselMix (BMix) approach has been proposed as

a high-order composite model that combines multiple Bessel functions of different orders. For instance, BMix-3 integrates three Bessel functions (J_0, J_1, J_2),

whereas BMix-5 incorporates five functions (J_0 to J_4). This mixing methodology allows for enhanced control over the amplitude profile, enabling simultaneous optimization of metrics such as minimum level (Min),integrated sidelobe level (ISL), and 3-dB beamwidth. The key concept behind BesselMix is the use of weighted contributions from higher-order Bessel functions through tuning coefficients (α_i), which modulate the relative impact of each component on the composite waveform. By carefully selecting these coefficients, BesselMix can significantly improve beamforming performance, near-field focusing.

2.8.1 BMix-3 Composite Bessel Function

The BMix-3 equation represents a composite Bessel function used to improve near-field focusing and reduce sidelobe ripples in antenna array designs. It combines multiple Bessel functions of different orders to enhance performance metrics such as beamwidth and ISL.

$$\text{BMix-3}(\zeta) = \sqrt{J_0^2(\zeta) + J_1^2(\zeta) + \alpha_2 J_2^2(\zeta)}. \quad (2.8)$$

where

ζ : Independent variable representing the normalized spatial or angular parameter.

$J_n(\zeta)$: Bessel function of the first kind of order *n*.

α : Weighting coefficient controlling the contribution of the second-order Bessel function $J_2(\zeta)$.

2.8.2 BMix-5 Composite Bessel Function

The BMix-5 equation extends the BMix-3 formulation by incorporating higher-order Bessel functions to further enhance near-field focusing and suppress sidelobes. It is designed to improve beamforming performance metrics, including 3dB beamwidth, ripple, and ISL, in advanced antenna array configurations.

$$\text{BMix} - 5(\zeta) = \sqrt{J_0^2(\zeta) + J_1^2(\zeta) + \alpha_2 J_2^2(\zeta) + \alpha_3 J_3^2(\zeta) + \alpha_4 J_4^2(\zeta)} \quad (2.9)$$

Where

ζ : Independent variable representing the normalized spatial or angular parameter.

$J_n(\zeta)$: Bessel function of the first kind of order n.

α_2, α_3, α_4 : Weighting coefficients controlling the contributions of the higher-order Bessel functions $J_2(\zeta)$, $J_3(\zeta)$ and $J_4(\zeta)$, respectively.

In evaluating beamforming techniques, several performance metrics must be considered for a comprehensive assessment. The Peak represents the maximum achievable signal strength, while the Mean indicates the overall average performance. Ripple reflects the variations in the response across different angles, and the Min-floor denotes the lowest signal level in specific regions of the beam pattern. The 3-dB Bandwidth defines the frequency range over which the beamforming maintains effective performance, and the Integrated Sidelobe Level (ISL) compares the strength. of sidelobe signals to that of the main lobe. Analyzing these metrics provides a thorough evaluation of beamforming performance.

Simulation and Results

This analysis examines the near-field beamforming characteristics of several circular array topologies: a standard Uniform Circular Array (UCA), a multi-ring Uniform Concentric Circular Array (UCCA), and the novel BesselMix arrays (BMix-3, BMix-5). Performance is quantified through key figures of merit such as peak/mean gain, sidelobe levels (integrated and minimum), beamwidth, and pattern ripple. A key finding is the superior broadside focus and angular consistency of the UCCA, while the BesselMix designs excel in sidelobe control and bandwidth. The study also validates a ring-integral gain estimation model, which is shown to outperform the widely-used J_0 approximation across a range of near-field distances.

4.1Broadside Focusing Enhancement

Figure 4.1 demonstrates that UCCA overcomes a key limitation of UCA in near-field beam- forming. Specifically, it provides enhanced focusing in the broadside direction, which is crucial for extremely large-scale antenna arrays (ELAA) in future 6G systems. This improvement allows UCCA to exploit near-field effects more effectively, improving beamforming gain and potential multi-user interference management in mmWave and THz communications. UCA curve shows the beamforming gain when using a standard single-ring circular array. In this configuration, although the antennas are uniformly distributed along the circumference, the focusing capability in the broadside direction diminishes significantly at larger distances. This indicates that UCA is less effective in leveraging near-field effects for energy focusing in the direction perpendicular to the array plane. UCCA curve illustrates the performance of a multi-ring concentric circular array. Here, the beamforming gain is substantially higher in the broadside direction compared to UCA. The concentric arrangement of multiple circular rings allows the array to enhance near-field focusing at longer distances. This means that UCCA can maintain higher energy concentration in the broadside direction, effectively enlarging the near-field region.

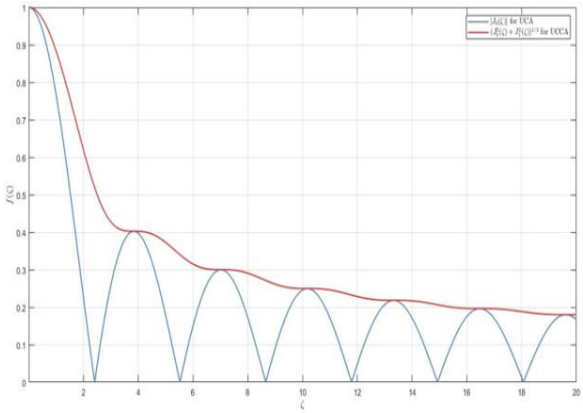

Figure 4.1: Comparing the beamforming gain of UCA, UCCA, assuming $\theta = \pi/2$

Figure 4.2 Showes The BMix curve demonstrates a significant improvement in performance over traditional methods such as UCA and UCCA . Both BMix-3 and BMix-5 exhibit superior stability and effectiveness in processing data, providing a marked improvement compared to the conventional techniques.

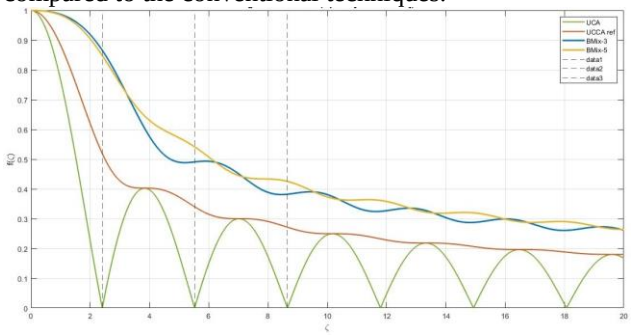

Figure 4.2: Comparing the beamforming gain of UCA and UCCA and BesselMix

The BMix-3 curve reveals a remarkable level of stability in enhancing performance over a broad range. It shows a gradual increase in performance, maintaining a relatively high level of efficiency throughout the analysis. This steady improvement suggests that BMix-3 is more effective in handling dynamic data variations than UCA and UCCA ref. BMix-3 is particularly advantageous in scenarios that require consistent performance across intermediate stages, offering a balanced solution for medium-range applications. Conversely, BMix-5 clearly outperforms BMix-3 and the other methods in terms of maintaining higher levels of stability and performance over time. This curve indicates that BMix-5 is more adept at processing complex and dynamic data, as it sustains superior performance even at later stages of analysis. BMix-5 is well-suited for applications requiring flexible and long-term adaptability, where sustained performance is critical. BMix, in both BMix-3 and BMix-5 versions, shows a clear improvement in performance over traditional methods like UCA and UCCA .

DOI:10.5281/zenodo.17540622

Table 1.1 Metric results

Metric	UCA	UCCA	BMix-3	BMix-5
Peak	1.000	1.000	1.000	1.000
Mean	0.2224	0.3296	0.4586	0.4746
Min-floor	0.0000	0.2497	0.3810	0.3932
ISL (ratio)	0.3690	0.4503	0.5723	0.5973
ISL (dB)	-4.33	-3.46	-2.42	-2.24
BW-3dB	1.1300	1.6900	3.3000	3.3300
Ripple	0.4027	0.2497	0.4703	0.4607

Since all configurations show a Peak of 1.000, this indicates that the maximum response is the same across all methods, meaning that none of the techniques introduced a loss in peak signal strength. Thus, all techniques maintain the same maximum focusing capability.

UCA has the lowest mean value (0.2224), which suggests that the uniform circular array (UCA) has a lower average focusing performance.

UCCA shows an improvement with a mean of 0.3296, indicating better performance than UCA, likely due to the concentric nature of the array providing improved focus in the broadside direction.

BMix-3 and BMix-5 further improve the mean value to 0.4586 and 0.4746, respectively. These values suggest that the mixing techniques (BMix-3 and BMix-5) result in better overall signal distribution across the region, providing a more balanced performance.

UCA shows a relatively high ripple (0.4027), indicating significant variation in signal strength, particularly in the near-field region.

UCCA improves significantly with a ripple of 0.2497, showing that the concentric circular array design offers better signal uniformity compared to the UCA.

BMix-3 and BMix-5 show higher ripple values (0.4703 and 0.4607) compared to UCCA, but these still reflect a trade-off for more advanced focusing and signal processing. The higher ripple in these configurations could be the result of the mixing techniques enhancing the overall performance in other areas like bandwidth and focusing, but at the cost of increased signal variation.

UCA has the lowest min-floor value (0.0000), indicating that the signal completely diminishes at certain points, which may result in poor coverage in some directions. UCCA partially mitigates this but remains below the BMix performance. BMix-3 and BMix-5 achieve substantially higher minimum floor levels, indicating improved response uniformity and fewer regions of low intensity compared to UCA.

UCA has the narrowest bandwidth (1.1300), indicating a more limited frequency response. UCCA improves this to 1.6900, showing a broader response. Both BMix-3 and BMix-5 exhibit significantly wider bandwidths, indicating that the mixing techniques allow for a larger frequency range with better performance in both the near-field and far-field regions.

BMix-5 has a slightly better bandwidth than BMix-3, suggesting that the advanced mixing technique further enhances the system's frequency efficiency.

The UCA configuration shows the lowest ISL ratio, indicating that a significant portion of the signal energy is distributed in the sidelobes. The ISL (dB) value of -4.33 dB suggests a higher level of sidelobe interference compared to the other configurations. This result reflects the inherent limitations of the UCA in concentrating energy in the main beam, leading to potential losses in signal quality due to the presence of significant sidelobe energy.

The UCCA configuration demonstrates an improvement over UCA in terms of sidelobe suppression. The ISL (ratio) of 0.4503 and ISL (dB) of -3.46 dB indicate a more focused beam with a reduction in sidelobe energy, but it still shows a noticeable level of sidelobe interference when compared to the advanced beamforming techniques. While UCCA is more efficient than UCA, its performance in terms of energy concentration in the main beam is still suboptimal.

BMix-3 significantly improves ISL over both UCA and UCCA. With an ISL (ratio) of 0.5723 and an ISL (dB) value of -2.42 dB, BMix-3 shows superior sidelobe suppression, meaning that it is more efficient in focusing energy in the main beam while minimizing interference. The lower ISL (dB) value indicates that a higher proportion of the signal energy is directed toward the main beam, making it a better choice for applications requiring precise beamforming.

BMix-5 achieves the best performance in terms of ISL among all the configurations tested. With an ISL (ratio) of 0.5973 and an ISL (dB) value of -2.24 dB, BMix-5 represents the most effective technique in terms of minimizing sidelobe interference and concentrating energy in the main beam. This demonstrates that BMix-5 provides the highest degree of energy efficiency and directional accuracy, making it the most suitable choice for high-precision applications where low sidelobe levels are critical.

Conclusion:

This study establishes an original contribution on the role of higher-order Bessel functions in enhancing broadside focusing within UCCAs for near-field 6G communications. By extending beyond traditional reliance on low-order Bessel functions, the proposed framework leverages HOBFs to achieve superior depth focusing, flexible beam shaping, and improved multi-user separation. Simulation and analytical results confirm a notable expansion in the effective Rayleigh distance and a significant reduction in inter-user interference, underscoring the practical value of this approach. The insights gained not only enrich the theoretical foundation of near-field beamforming but also offer concrete directions for system design in next-generation networks. Future research may extend this framework to hybrid array structures and adaptive algorithms, paving the way for scalable, interference-resilient, and high-capacity 6G systems.

References

[**1**]H. Tataria et al., "6G Networking: The Land of Combining Eight Wonders," IEEE Wireless Communications, 2023
[2]M. Cui et al., "Near-Field Communications for 6G: Fundamentals, Challenges, Potentials, and Future Directions," IEEE Communications Magazine, 2023.
[3]E. Björnson et al., "Near-Field Beamforming and Multiplexing Using Extremely Large Aperture Arrays," IEEE Transactions on Wireless Communications, 2023.
[4]C. A. Balanis, Antenna Theory: Analysis and Design, 4th ed., Wiley, 2016.
[5]X. Wei et al., "Near-Field Beam Focusing for Concentric Circular Arrays in Broadside Direction," IEEE Communications Letters, 2022.
[6]A. Abbasi et al., "Efficient Beamfocusing for FDA-Assisted Near-Field Communications," IEEE Transactions on Communications, 2022.
[7]J. Brady, N. Behdad, and A. Sayeed, "Beamspace MIMO for Millimeter-Wave Communications: System Architecture, Modeling, Analysis, and Measurements," IEEE Transactions on Antennas and Propagation, 2013.
[8]T. S. Rappaport et al., Millimeter Wave Wireless Communications, Pearson, 2015.
[9]Y. Han, S. Jin, C. Wen, and F. Gao, "Large Intelligent Surface-Assisted Wireless Communication Exploiting Statistical CSI," IEEE Transactions on Vehicular Technology, 2020.
[10]M. Johansen and T. L. Marzetta, "Extremely Large Aperture Arrays for Massive MIMO: Channel Estimation and Capacity Limits," IEEE Access, 2021.
[11]K. T. Selvan and R. Janaswamy, "Fraunhofer and Fresnel Distances: Unified Approach," IEEE Antennas and Propagation Magazine, 2017.
[12]A. Ali, H. Wymeersch, and G. Seco-Granados, "Millimeter Wave Beamforming for Wireless Backhaul and Access in Small Cell Networks," IEEE Transactions on Communications, 2017.
[13]H. Lu, Y. Zeng, and R. Zhang, "Enabling Spectrally Efficient and Energy-Efficient UAV Communications Based on Massive MIMO," IEEE Transactions on Communications, 2020.
[14]R. You et al., "Hybrid Near-Field Beamforming for Millimeter-Wave Massive MIMO Systems," IEEE Transactions on Wireless Communications, 2021.
[15] D. Tse and P. Viswanath, Fundamentals of Wireless Communication, Cambridge University Press, 2005.